

Lawrence Berkeley National Laboratory

LBL Publications

Title

Metal-Free Peralkylation of the closo-Hexaborate Anion

Permalink

<https://escholarship.org/uc/item/4qm804nc>

Journal

Organometallics, 36(6)

ISSN

0276-7333

Authors

Axtell, Jonathan C
Kirlikovali, Kent O
Jung, Dahee
[et al.](#)

Publication Date

2017-03-27

DOI

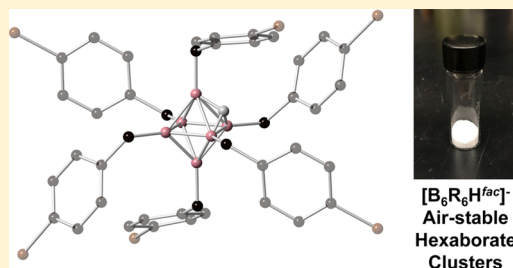
10.1021/acs.organomet.7b00078

Peer reviewed

Metal-Free Peralkylation of the *closo*-Hexaborate AnionJonathan C. Axtell,[†] Kent O. Kirlikovali,[†] Dahee Jung,[†] Rafal M. Dziezic,[†] Arnold L. Rheingold,[‡] and Alexander M. Spokoyny^{*,†,§}[†]Department of Chemistry and Biochemistry, University of California, Los Angeles, 609 Charles E. Young Drive East, Los Angeles, California 90095, United States[‡]Department of Chemistry and Biochemistry, University of California, San Diego, 9500 Gilman Drive, La Jolla, California 92093, United States[§]California NanoSystems Institute, University of California, Los Angeles, California 90025, United States

Supporting Information

ABSTRACT: The synthesis of fully alkylated *closo*-hexaborate dianions is reported. The reaction of $[\text{NBu}_4][\text{B}_6\text{H}_6^{\text{fac}}]$, benzyl bromide, and triethylamine under microwave heating conditions affords persubstituted $[\text{NBu}_4][\text{B}_6(\text{CH}_2\text{Ar})_6\text{H}^{\text{fac}}]$ ($\text{Ar} = \text{C}_6\text{H}_5$, 4- $\text{Br-C}_6\text{H}_4$), which have been isolated and characterized by NMR spectroscopy, mass spectrometry, single-crystal X-ray diffraction, and other spectroscopic techniques. Electrochemical studies of these clusters reveal an irreversible one-electron oxidation, likely indicating degradative cage rupture. The observed metal-free alkylation is proposed to proceed as a consequence of the pronounced nucleophilic character of the hexaborate anion. This work represents the first example of a perfunctionalized hexaborate cluster featuring B–C bonds.



INTRODUCTION

Many polyhedral boron clusters have been shown to exhibit enhanced stability relative to more commonly encountered tricoordinate boranes. This stability has been ascribed to the unique bonding arrangement and three-dimensional aromatic character of these polyhedral clusters.¹ For example, the 12-membered, dodecaborate B_{12} -based cluster core exhibits extreme kinetic stability, remaining intact under strongly acidic, oxidizing, and basic conditions, as well as heating in air beyond 600 °C.² Partial and exhaustive functionalization of this cluster core can furnish unique molecular scaffolds which are potentially useful for a wide range of applications³ including, but not limited to, photoactive materials, polymers, electrolytes, catalysts, therapeutics, and diagnostic agents in biomedicine.⁴ The ability to design and tune these molecules remains crucial for producing desirable properties and reactivity.

In general, two main approaches to persubstituted group 13 polyhedral clusters exist. The first involves the assembly of prefunctionalized fragments to form the desired cluster-based motif (Figure 1, route A). This approach has frequently been utilized in the context of group 13 clusters—most notably in the seminal work by Schnöckel—and to a lesser degree with small boron-based clusters.⁵ The second approach involves first the synthesis of an unsubstituted cluster core precursor, which is then elaborated with functional groups (Figure 1, route B). This latter approach has been applied almost exclusively in boron cluster chemistry,⁴ particularly with the icosahedral boron clusters. This is not surprising, given that unfunctionalized icosahedral boranes are significantly more stable than

Figure 1. Two general approaches for synthesizing substituted group 13 clusters. Route A involves the combination of substituted fragments “E–R” of one or several types to form the desired molecule. Route B employs a preformed cluster and an external functionality “R” to form the same desired framework.

their heavier group 13 congeners⁶ and thus can serve as molecular precursors for the latter method of synthesis.

Beyond icosahedra, other polyhedral boron clusters are known,⁷ and in contrast to the well-established chemistry of the $\text{B}_{12}\text{H}_{12}^{2-}$ dianion and its derivatives, the chemistry of the *closo*-hexaborate dianion, $\text{B}_6\text{H}_6^{2-}$ —the smallest of the known deltahedral 3D aromatic boron clusters—has received much less attention. Predicted⁸ in 1954 and isolated⁹ in 1964, the $\text{B}_6\text{H}_6^{2-}$ dianion, which is stable under ambient conditions in both the solid and solution state, was quickly shown to be rather different from its icosahedral relative. The pioneering work of Preetz¹⁰ revealed the apparent nucleophilic character of the hexaborate clusters to be significantly more pronounced than that of the $\text{B}_{12}\text{H}_{12}^{2-}$ species. This observation led to some

Received: February 2, 2017

Published: March 10, 2017

early examples demonstrating that $B_6H_6^{2-}$ can undergo *partial* substitution with carbon-based electrophiles to form B–C bonds; similar reactions with the dodecaborate scaffold have not been disclosed. To date, *peralkylation* of the hexaborate cluster has never been accomplished. Here we disclose the synthesis and properties of the first peralkylated hexaborate clusters, $B_6(CH_2Ar)_6^{2-}$ ($Ar = C_6H_5$, 4-Br- C_6H_5), generated as a consequence of the nucleophilic character of the hexaborate dianion.

RESULTS AND DISCUSSION

Preetz and co-workers previously disclosed¹¹ several examples of alkylated hexaborate clusters of the type $B_6R_nH_{6-n}^{2-}$ ($n = 1–3$, $R = \text{alkyl}$), and it was ultimately suggested that alkylation would not proceed beyond three substitutions. B–C bond formation is thought to occur with concomitant migration of the terminal H from the B vertex to an adjacent *face* of the hexaborate cluster. This facial proton (H^{fac}) mitigates the nucleophilicity of the cluster and must be removed with base for further substitutions to occur. In the examples reported by Preetz, it was concluded that that removal of H^{fac} was not possible beyond three B–C bond formations.¹⁰ Given our recent report¹² of microwave-assisted functionalization of $B_{12}(OH)_{12}^{2-}$ with alkyl electrophiles, which could afford densely functionalized clusters within minutes, we wondered whether similar reaction conditions might produce fully functionalized $B_6R_6^{2-}$ frameworks, bypassing previously encountered limitations.

Treatment of $[NBu_4][B_6H_6H^{fac}]$ with 30 equiv. of benzyl bromide and Hünig's base in CH_3CN under microwave heating conditions led to the formation of a new species displaying a single, broad resonance at $\delta -7.6$ in the ^{11}B NMR spectrum. Further optimization of the reaction conditions permitted the isolation of $[NBu_4][B_6(CH_2C_6H_5)_6H^{fac}]$ (**1a**) after workup in 65% yield (Figure 2A and the Supporting Information). The facial proton in **1a** can be identified by its characteristic upfield shift at $\delta -3.8$ in the 1H NMR spectrum. This assignment is consistent with previous spectroscopic and structural studies^{10,13} of analogous unfunctionalized and partially functionalized B_6 -based clusters as well as computational studies in which electron density maxima are found at each face of the B_6 cluster.¹⁴ Complete boron vertex substitution, which occurs in the absence of metal catalysis, is also strongly suggested by the disappearance of characteristic terminal B–H stretching vibrations at $\sim 2400\text{ cm}^{-1}$ in the infrared (IR) spectrum of purified **1a** (Figure 2B).

X-ray diffraction of crystals of **1a** revealed significant disorder due to “wagging” of the benzyl substituents, which was also observed for $[B_6H_5(CH_2Ph)]^{2-}$.¹⁵ We therefore employed a functionalized benzyl electrophile in an attempt to impart greater order and crystallinity to the desired persubstituted product. Treatment of $[NBu_4][B_6H_6H^{fac}]$ with 4-bromobenzyl bromide under conditions otherwise identical with those used to synthesize **1a** similarly affords a compound that displays a single broad peak in the ^{11}B NMR spectrum at $\delta -7.6$ and an IR spectrum consistent with **1a** (Figure 2). Upon workup, perfunctionalized **1b** is afforded in 48% yield as a white, air-stable solid.

An X-ray diffraction study was carried out on single crystals of **1b** grown from a cooling solution of **1b** in boiling ethanol. **1b** crystallizes in the $P2_1$ space group with two independent ion pairs in the asymmetric unit (Figure 3). One NBu_4^+ counterion

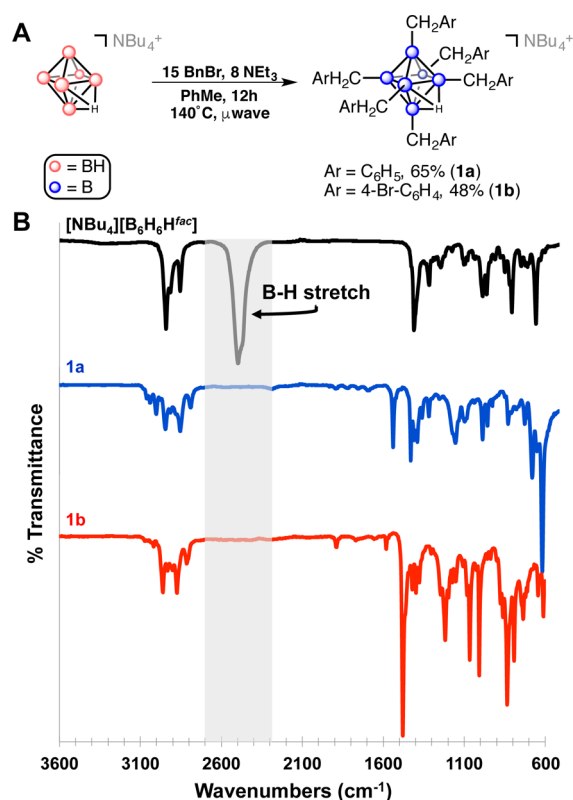


Figure 2. (A) Synthetic scheme for **1a,b** from $B_6H_6^{2-}$. (B) IR spectra of $[NBu_4][B_6H_6H^{fac}]$, and **1a,b**. The absence of stretching vibrations from ~ 2100 to 2600 cm^{-1} for **1a,b** suggests a lack of terminal B–H bonds and complete cluster substitution.

is detected per cluster, supporting the proposed facially protonated monoanion and consistent with the 1H NMR data.

While definitive location of the facial proton (H^{fac}) proved difficult, its position can be tentatively assigned on the basis of the bond metrics of the B_6 -based core. The B1–B2–B3 face contains three of the four longest B–B distances in the cluster

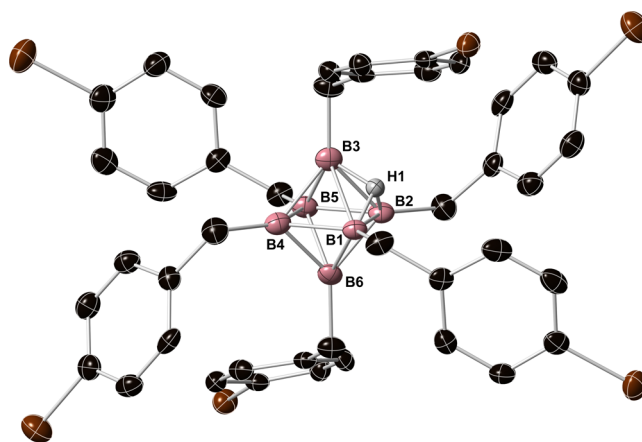


Figure 3. B_6 -based component of the single-crystal X-ray structure of **1b**. Benzyl protons and the NBu_4 counterion are omitted for clarity. H1 (H^{fac}) was placed at the B1–B2–B3 face and refined. Selected distances (\AA): B1–B2, 1.817(8); B1–B3, 1.818(8); B1–B4, 1.725(9); B1–B6, 1.729(8); B2–B3, 1.788(8); B2–B5, 1.713(9); B2–B6, 1.739(8); B3–B4, 1.779(9); B3–B5, 1.769(8); B4–B5, 1.822(8); B4–B6, 1.746(8); B5–B6, 1.764(8). Thermal ellipsoids (except for H1) are plotted at 50% probability.

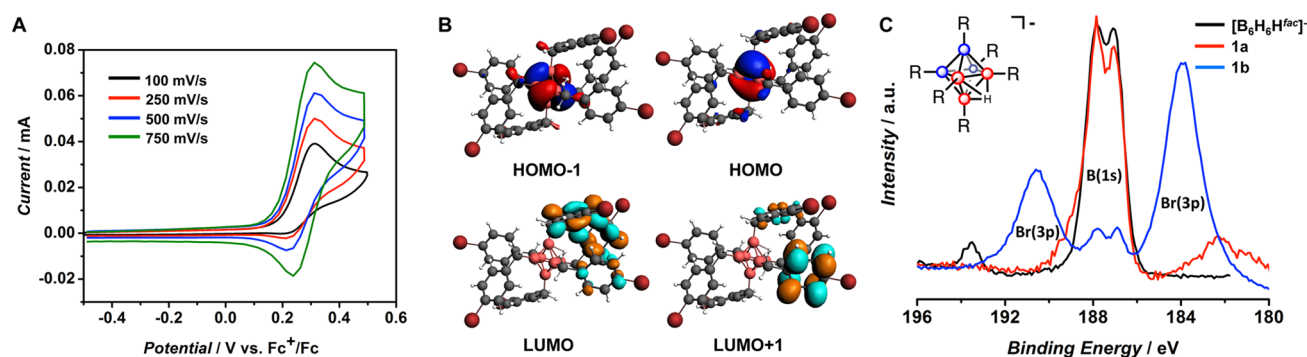


Figure 4. (A) Cyclic voltammogram of **1a** in CH_3CN . Faster scan rates reveal the pseudoreversibility of the 1[−]/0 redox couple. (B) Kohn–Sham representations derived from the DFT analysis of the frontier molecular orbitals of the anionic component of **1b**, $[\text{B}_6(\text{CH}_2\text{-4-Br-C}_6\text{H}_4)_6]^-$. (C) Normalized X-ray photoelectron spectra of $[\text{NBu}_4][\text{B}_6\text{H}_6\text{H}^{\text{fac}}]$ and **1a,b**. The B(1s) region shows two different boron environments: those in which bonding interactions to H^{fac} are present (red spheres) and absent (blue spheres).

(1.818, 1.818, and 1.789 Å), which are large in comparison to the average of all other B–B distances, 1.725 Å (range 1.713–1.824 Å). We therefore suggest that H^{fac} is bound to this face of the cage in the solid state. This assignment is consistent with previous reports.^{13,16} All B–C bonds range from 1.592 to 1.601 Å, which are consistent with the B–C bond distances in previously reported monobenzylated clusters.¹⁵

While the homo- and heteroleptic perhalogenation (Cl, Br, I) of $\text{B}_6\text{H}_6^{2-}$ has been reported,¹⁷ **1a,b** are the first molecules of their type in which carbon-based substituents are bound to each vertex of the hexaborate cage. Indeed, the only other reports of perfunctionalized hexaborate clusters are the charge-neutral $\text{B}_6(\text{NR}_2)_6$ species (R = Me, Et).¹⁸ In contrast to **1a,b**, the $\text{B}_6(\text{NR}_2)_6$ clusters irreversibly open into cyclic constitutional isomers on heating. We suggest that the formation of **1a,b** proceeds via a simple $\text{S}_{\text{N}}2$ mechanism: $\text{B}_6\text{H}_6^{2-}$, which contains electron density maxima at each face of the octahedron and is generated by deprotonation of the B_6H_7^- anion under the reaction conditions, is proposed to behave as the nucleophile, displacing the primary halide of the benzyl electrophile, forming a B–C bond. The hydride bound to the boron vertex undergoing substitution shifts to an adjacent face (see H^{fac} in Figure 3) in concert with this B–C bond formation and must be deprotonated by base in order for further substitutions to occur. At this point, however, single-electron pathways cannot be ruled out.

Perhalogenated clusters $\text{B}_6\text{X}_6^{2-}$ (X = Cl, Br, I), mixed halogen clusters $\text{B}_6\text{X}_n\text{X}'_{6-n}^{2-}$ (X = F, Cl, Br, I; for X = F, $n = 1$), and $\text{B}_6\text{X}_3\text{R}^{2-}$ (R = alkyl) were previously shown to exhibit redox behavior.¹⁹ To determine the electrochemical behavior of **1a,b**, cyclic voltammetry (CV) studies were conducted. Solutions of **1a,b** in anhydrous CH_3CN display apparent irreversible one-electron-oxidation waves at 0.32 and 0.46 V vs Fc/Fc^+ , respectively (see Figure 4A and the Supporting Information). The observed redox irreversibility is consistent with previous reports of hexaborate cluster decomposition under oxidizing conditions (*vide infra*).^{10,20} The anodic shift in the oxidative peak potential between **1a** and **1b** is likely due to the slightly more electron withdrawing nature of the benzyl substituents in **1b**; similar substituent effects have been observed in hexaborate¹⁹ and dodecaborate systems.¹²

As the scan rate is incrementally raised from 100 mV/s to 750 mV/s for **1a**, a reverse reductive wave becomes more pronounced (Figure 4A). These data suggest that the benzyl substituents of **1a** stabilize the transient neutral $\text{B}_6(\text{CH}_2\text{C}_6\text{H}_5)_6\text{H}^{\text{fac}}$ toward decomposition relative to $[\text{NBu}_4]$ -

$[\text{B}_6\text{H}_6\text{H}^{\text{fac}}]$ (see the Supporting Information). One possible explanation lies in the peripheral benzyl substituents: the steric bulk of these groups likely prevents oxidative dimerization, which is known to occur with $\text{B}_6\text{H}_6^{2-}$.^{19c,21} Similar stabilizing effects by boron cluster substitution have been suggested by Michl in the context of icosahedral carba-*closo*-dodecaborates.²² Therefore, the irreversibility of this redox couple must originate from some other mode of decomposition, likely cage degradation (*vide infra*).²³ We attribute the absence of redox reversibility at higher scan rates in the case of **1b** to electronic differences in the benzyl substituents in comparison to **1a**, which may destabilize the cluster to a greater degree upon oxidation. Identification of the decomposition products of these oxidative processes is currently ongoing.

The electronic structure of **1b** was probed using density functional theory (DFT) at the BP86-D3/TZP level of theory, and the frontier molecular orbital diagrams obtained from this study are presented in Figure 4B. In agreement with previous computational studies of $[\text{B}_6\text{H}_6]^{2-}$,¹⁴ the highest occupied molecular orbital (HOMO) and the HOMO-1 are found to be delocalized across the eight faces of the octahedron. In contrast, the lowest unoccupied molecular orbital (LUMO) and the LUMO+1 are primarily located on the benzyl moieties. The observed decomposition of **1a,b** under anodic electrochemical potentials (*vide supra*) is consistent with removal of an electron from the cluster-based HOMO, resulting in kinetic destabilization due to an overall reduction in cage bonding character and 3D aromaticity.²⁴

Intrigued by the unique bonding structure of **1a,b**, we performed X-ray photoelectron spectroscopy (XPS) measurements to further probe the electronic landscape of the B_6 -based core (Figure 4C). The B(1s) binding energy for **1a,b** and unfunctionalized cluster $[\text{NBu}_4][\text{B}_6\text{H}_6\text{H}^{\text{fac}}]$ is observed to be ~ 187 eV, which is consistent with B(1s) binding energies previously measured for substituted icosahedral dodecaborate clusters¹² and with the B(1s) binding energy of boron species in general.²⁵ The degree and type of substitution (H vs alkyl; benzyl vs 4-bromobenzyl) do not seem to strongly affect the binding energy. Interestingly, we find two maxima in the 187 eV region for all compounds at 187.1 and 187.9 eV (Figure 4C). We attribute this observation to the existence of two distinct boron environments in $[\text{NBu}_4][\text{B}_6\text{H}_6\text{H}^{\text{fac}}]$ and **1a,b**: one triangular face contains three boron atoms which share bonding interactions to H^{fac} ; the other three atoms of the octahedron do not contain a $\text{B}\cdots\text{H}^{\text{fac}}$ interaction. Since higher binding energies roughly correlate with degree of oxidation, we

suggest that, given the reduction in electron density from one face of the octahedron by H^+ in the form of a covalent bonding interaction relative to B–H units which do not contain this interaction, the peak of higher binding energy corresponds to the set of boron atoms binding $B\cdots H^{ac}$. To our knowledge, this is the first XPS study of a hexaborate species.

CONCLUSION

In summary, we have found that the perfunctionalization of the hexaborate dianion is achievable via treatment with benzyl halides, resulting in the formation of six B–C bonds per cluster. These results suggest that the hexaborate cluster may be potentially (per)functionalized with other electrophiles to form B–R bonds of varying types without the need for metal-based catalysis. The newly reported compounds, which are stable solids under ambient conditions, exhibit irreversible electrochemical oxidations, likely the result of cage degradation, ultimately suggesting a differing reactivity from the peralkylated dodecaborate ($B_{12}R_{12}^{2-/-}$) species.^{4b–d}

EXPERIMENTAL SECTION

General Considerations. All experiments were set up in a nitrogen-filled glovebox unless otherwise noted. Toluene (C_7H_8) used for reactions set up in a glovebox to form **1a,b** and acetonitrile (CH_3CN) used for cyclic voltammetry were sparged with argon and passed through activated alumina prior to use. All other solvents were used as received. “Ambient conditions” for this paper refer to room temperature (20–25 °C) and uncontrolled laboratory air.

Materials. Deuterated solvents were purchased from Cambridge Isotope Laboratories and were stored over 3 Å molecular sieves under ambient conditions. Hexanes, toluene (C_7H_8), ethanol (EtOH), and methylene chloride (CH_2Cl_2) were purchased from Sigma-Aldrich. Celite and silica gel (Grade 60, 230–400 mesh) were purchased from Fisher Scientific. 4-Bromobenzyl bromide, tetrabutylammonium hexafluorophosphate, tetrabutylammonium hydroxide (40 wt % in H_2O), tetrabutylammonium bromide (NBu_4Br), potassium phosphate (tribasic; K_3PO_4), and ferrocene were purchased from Sigma-Aldrich and used as received. Benzyl bromide was purchased from Sigma-Aldrich and was filtered through a silica plug and stored over 3 Å molecular sieves; for experiments conducted in the glovebox, the silica-treated benzyl bromide was carried through two freeze–pump–thaw cycles before it was brought into the glovebox. Triethylamine was purchased from Sigma-Aldrich and used as received; for experiments conducted in the glovebox, the triethylamine was carried through two freeze–pump–thaw cycles before it was brought into the glovebox. $[NBu_4][B_6H_7]$ was obtained according to the procedure by Kabbani.²⁶ Note: use of fresh $NaBH_4$ and $BF_3\cdot Et_2O$ is essential for good yields of $[NBu_4][B_6H_6H^{ac}]$. In our hands, we obtain $[NBu_4][B_6H_6H^{ac}]$ instead of the reported $[(NBu_4)_2][B_6H_6]$; the $B_6H_6^{2-}$ anion is strongly basic and acquires protons under ambient conditions or even from solvent with trace water. Preetz has also remarked on this property.¹⁰ However, we find $[NBu_4][B_6H_6H^{ac}]$ to be an acceptable starting material for the synthesis of the compounds outlined below.

Synthetic Procedures. Note: due to the acid sensitivity of the hexaborate clusters, trace acid occasionally found in $CDCl_3$ must be neutralized to ensure product stability in solution. The reported reactions may be set up outside the glovebox and likewise furnish **1a,b** with only slightly diminished yields.

$[NBu_4][B_6(CH_2C_6H_5)_6H^{ac}]$ (**1a**). In a nitrogen-filled glovebox, $[NBu_4][B_6H_6H^{ac}]$ (50 mg, 0.140 mmol) was charged in a 10 mL microwave reactor vial followed by 1 mL of C_7H_8 . Note: the mixture is poorly soluble in C_7H_8 at room temperature. Then, trimethylamine (142 μ L, 1.40 mmol) was added, followed by benzyl bromide (250 μ L, 2.10 mmol). The Teflon cap was affixed, and the vial was brought out of the box and set to heat in the microwave for 12 h at 140 °C. After 12 h, a translucent slurry was observed that had a slight blue tint. The slurry was diluted with hexanes (~6 mL), and the mixture was

manually stirred to further precipitate a white solid. The solid was filtered over Celite and washed thoroughly with hexanes. The solid was then washed through the Celite pad into a separate receiving flask with CH_2Cl_2 . This filtrate was charged to a separatory funnel containing ~25 mL of a 0.15 M NBu_4OH (40 wt % in H_2O) aqueous solution. The organic layer was washed twice with this solution, isolated, dried over Na_2SO_4 , and filtered through Celite. The filtrate was dried in vacuo. The residue (which may be slightly blue) was then charged with ~5 mL of EtOH to precipitate a white solid. The mixture was stirred vigorously for ~20 min and was subsequently set in a –15 °C freezer for 3–4 h. The solid was then isolated on a fritted funnel and washed with cold (–15 °C) EtOH. The white solid product was dried under vacuum (78 mg, 65%). 1H NMR ($CDCl_3$, 500 MHz): δ 7.04 (t, 12H, Ar), 6.88 (t, 6H, Ar), 6.78 (d, 12H, Ar), 2.46 (m, 8H, $[N(CH_2(CH_2)_2CH_3)_4]^+$), 1.80 (s, 12H, CH_2Ar), 1.26 (m, 16H, $[N(CH_2(CH_2)_2CH_3)_4]^+$), 1.18 (t, 12H, $[N(CH_2(CH_2)_2CH_3)_4]^+$), –3.54 (br s, 1H, H^{ac}). ^{13}C NMR ($CDCl_3$, 125 MHz): δ 149.65, 128.99, 127.31, 122.05, 58.29, 23.70, 21.33, 19.71, 13.83. ^{11}B NMR ($CDCl_3$, 160 MHz): δ –6.19. Mass spectrometry (ES^-): expected monoisotopic peak (m/z) for $[B_6C_{42}H_{43}]^-$ 609.3960, found 609.3954.

$[NBu_4][B_6(CH_2-4-Br-C_6H_4)_6H^{ac}]$ (**1b**). In a nitrogen-filled glovebox, $[NBu_4][B_6H_6H^{ac}]$ (100 mg, 0.281 mmol) was charged in a 10 mL microwave reactor vial followed by 2 mL of C_7H_8 . Note: the mixture is poorly soluble in C_7H_8 at room temperature. Then, trimethylamine (313 μ L, 2.24 mmol) was added, followed by 4-bromobenzyl bromide (1.05 g, 4.21 mmol). The Teflon cap was affixed, and the vial was brought out of the box and set to heat in the microwave for 12 h at 140 °C. After 12 h, a white slurry was observed. The slurry was diluted with hexanes (~6 mL), and the mixture was manually stirred to further precipitate a white solid. The solid was filtered over Celite and washed thoroughly with hexanes. The solid was then washed through the Celite pad into a separate receiving flask with CH_2Cl_2 . This filtrate was charged to a separatory funnel containing ~25 mL of a 0.02 M $NBu_4Br/0.09$ M K_3PO_4 aqueous solution (500 mg of NBu_4Br and 2 g of K_3PO_4 in 100 mL of deionized H_2O). The organic layer was washed twice with this solution, isolated, dried over Na_2SO_4 , and filtered through Celite. The filtrate was dried in vacuo. The residue (which may be slightly yellow) was then charged with ~5 mL of EtOH to precipitate a white solid. The mixture was stirred vigorously for ~20 min and was subsequently set in a –15 °C freezer for 3–4 h. The solid was then isolated on a fritted funnel and washed with cold (–15 °C) EtOH. The white solid product was dissolved in boiling ethanol and allowed to recrystallize. The crystalline product was dried under vacuum (179 mg, 48%). 1H NMR ($CDCl_3$, 500 MHz): δ 7.17 (d, 12H, Ar), 6.57 (d, 12H, Ar), 2.64 (m, 8H, $[N(CH_2(CH_2)_2CH_3)_4]^+$), 1.75 (s, 12H, CH_2Ar), 1.31 (m, 16H, $[N(CH_2(CH_2)_2CH_3)_4]^+$), 1.03 (t, 12H, $[N(CH_2(CH_2)_2CH_3)_4]^+$), –3.75 (br s, 1H, H^{ac}). ^{13}C NMR ($CDCl_3$, 125 MHz): δ 148.32, 130.62, 130.28, 115.56, 58.68, 23.74, 20.49, 19.78, 13.82. ^{11}B NMR ($CDCl_3$, 160 MHz): δ –7.62. Mass spectrometry (ES^-): expected monoisotopic peak (m/z) for $[B_6C_{42}H_{37}Br_6]^-$ 1078.8551, found 1078.8588.

ASSOCIATED CONTENT

Supporting Information

The Supporting Information is available free of charge on the ACS Publications website at DOI: 10.1021/acs.organomet.7b00078.

Experimental and instrumentation details and NMR spectra for **1a,b** as well as supplementary electrochemical, DFT, and XPS data (PDF)

Crystallographic data (CIF)

Cartesian coordinates for the calculated structure (XYZ)

Cartesian coordinates for the calculated structure (XYZ)

AUTHOR INFORMATION

Corresponding Author

*E-mail for A.M.S.: spokoyny@chem.ucla.edu.

ORCID 

Alexander M. Spokoyny: 0000-0002-5683-6240

Notes

The authors declare no competing financial interest.

ACKNOWLEDGMENTS

A.M.S. thanks the UCLA Department of Chemistry and Biochemistry for start-up funds and the donors of the American Chemical Society Petroleum Research Fund for support (56562-DNI3). The authors thank Dr. Liban M. A. Saleh for useful discussions, Ms. Alice Phung for translation of German manuscripts, Dr. Greg Khitrov for assistance with mass spectrometry, and Dr. Robert Taylor for assistance with quantitative ^{13}C NMR studies.

REFERENCES

- (1) (a) King, R. B.; Rouvray, D. H. *Chemical Applications of Group Theory and Topology. 7. A Graph-Theoretical Interpretation of the Bonding Topology in Polyhedral Boranes, Carboranes, and Metal Clusters.* *J. Am. Chem. Soc.* **1977**, *99*, 7834–7840. (b) Aihara, J.-I. Three-Dimensional Aromaticity of Polyhedral Boranes. *J. Am. Chem. Soc.* **1978**, *100*, 3339–3342. (c) Bridgeman, A. J.; Empson, C. J. Detecting Delocalization. *New J. Chem.* **2008**, *32*, 1359–1367. (d) Housecroft, C. E.; Snaith, R.; Moss, K.; Mulvey, R. E.; O'Neill, M. E.; Wade, K. Cluster Bonding and Energetics of the Borane Anions, $\text{B}_n\text{H}_n^{2-}$ ($n = 5-12$): A Comparative Study Using Bond Length–Bond Enthalpy Relationships and Molecular Orbital Bond Index Calculations. *Polyhedron* **1985**, *4*, 1875–1881. (e) Zhao, M.; Gimarc, B. M. 3-Dimensional Hückel Theory for Cluster Compounds. *Inorg. Chem.* **1993**, *32*, 4700–4707. (f) King, R. B. Three-Dimensional Aromaticity in Polyhedral Boranes and Related Molecules. *Chem. Rev.* **2001**, *101*, 1119–1152.
- (2) (a) Pitochelli, A. R.; Hawthorne, M. F. Isolation of the icosahedral $\text{B}_{12}\text{H}_{12}^{2-}$ ion. *J. Am. Chem. Soc.* **1960**, *82*, 3228–3229. (b) Muettterties, E. L.; Balthis, J. H.; Chia, Y. T.; Knoth, W. H.; Miller, H. C. Chemistry of Boranes. VIII. Salts and Acids of $\text{B}_{10}\text{H}_{10}^{2-}$ and $\text{B}_{12}\text{H}_{12}^{2-}$. *Inorg. Chem.* **1964**, *3*, 444–451.
- (3) (a) Grimes, R. N. Boron Clusters Come of Age. *J. Chem. Educ.* **2004**, *81*, 657–672. (b) Kaim, W.; Hosmane, N.; Zališ; Maguire, J. A.; Lipscomb, W. N. Boron Atoms as Spin Carriers in Two- and Three-Dimensional Systems. *Angew. Chem., Int. Ed.* **2009**, *48*, 5082–5091.
- (4) (a) Núñez, R.; Tarrés, M.; Ferrer-Ugalde, A.; de Biani, F. F.; Teixidor, F. Electrochemistry and Photoluminescence of Icosahedral Carboranes, Boranes, Metallacarboranes, and Their Derivatives. *Chem. Rev.* **2016**, *116*, 14307–14378. (b) Peymann, T.; Knobler, C. B.; Khan, S. I.; Hawthorne, M. F. Dodecamethyl-*closo*-dodecaborate(2-). *Inorg. Chem.* **2001**, *40*, 1291–1294. (c) Peymann, T.; Knobler, C. B.; Hawthorne, M. F. An Icosahedral Array of Methyl Groups Supported by an Aromatic Borane Scaffold: The $[\text{closo-B}_{12}(\text{CH}_3)_{12}]^{2-}$ Ion. *J. Am. Chem. Soc.* **1999**, *121*, 5601–5602. (d) Peymann, T.; Knobler, C. B.; Hawthorne, M. F. An Unpaired Electron Incarcerated Within an Icosahedral Borane Cage: Synthesis and Crystal Structure of the Blue, Air-Stable $\{[\text{closo-B}_{12}(\text{CH}_3)_{12}]^{2-}\}^{\cdot-}$ Radical. *Chem. Commun.* **1999**, *20*, 2039–2040. (e) Ivanov, S. V.; Miller, S. M.; Anderson, O. P.; Solntsev, K. A.; Strauss, S. H. Synthesis and Stability of Reactive Salts of Dodecafluoro-*closo*-dodeca-borate(2-). *J. Am. Chem. Soc.* **2003**, *125*, 4694–4695. (f) Peryshkov, D. V.; Popov, A. A.; Strauss, S. H. Latent Porosity in Potassium Dodecafluoro-*closo*-dodecaborate(2-). Structures and Rapid Room Temperature Interconversions of Crystalline $\text{K}_2\text{B}_{12}\text{F}_{12}$, $\text{K}_2(\text{H}_2\text{O})_2\text{B}_{12}\text{F}_{12}$, and $\text{K}_2(\text{H}_2\text{O})_4\text{B}_{12}\text{F}_{12}$ in the Presence of Water Vapor. *J. Am. Chem. Soc.* **2010**, *132*, 13902–13913. (g) Nieuwenhuyzen, M.; Seddon, K. R.; Teixidor, F.; Puga, A. V.; Viñas, C. Ionic Liquids Containing Boron Cluster Anions. *Inorg. Chem.* **2009**, *48*, 889–901. (h) Boeré, R. T.; Derendorf, J.; Jenne, C.; Kacprzak, S.; Keßler, M.; Riebau, R.; Reidel, S.; Roemmele, T. L.; Rühle, M.; Scherer, H.; Vent-Schmidt, T.; Warneke, J.; Weber, S. On the Oxidation of the Three-Dimensional Aromatics $[\text{B}_{12}\text{X}_{12}]^{2-}$ ($\text{X} = \text{F}, \text{Cl}, \text{Br}, \text{I}$). *Chem. - Eur. J.* **2014**, *20*, 4447–4459. (i) Maderna, A.; Knobler, C. B.; Hawthorne, M. F. Twelffold Functionalization of an Icosahedral Surface by Total Esterification of $[\text{B}_{12}(\text{OH})_{12}]^{2-}$: 12(12)-Closomers. *Angew. Chem., Int. Ed.* **2001**, *40*, 1661–1664. (j) Zhang, Y.; Liu, J.; Duttwyler, S. Synthesis and Structural Characterization of Ammonio/Hydroxo Undecachloro-*closo*-Dodecaborates $[\text{B}_{12}\text{Cl}_{11}\text{NH}_3]^-/[\text{B}_{12}\text{Cl}_{11}\text{OH}]^{2-}$ and Their Derivatives. *Eur. J. Inorg. Chem.* **2015**, *2015*, 5158–5162. (k) Gu, W.; Ozerov, O. V. Exhaustive Chlorination of $[\text{B}_{12}\text{H}_{12}]^{2-}$ without Chlorine Gas and the Use of $[\text{B}_{12}\text{Cl}_{12}]^{2-}$ as a Supporting Anion in Catalytic Hydrodefluorination of Aliphatic C-F Bonds. *Inorg. Chem.* **2011**, *50*, 2726–2728. (l) Van, N.; Tiritiris, I.; Winter, R. F.; Sarkar, B.; Singh, P.; Duboc, C.; Muñoz-Castro, A.; Arratia-Pérez, R.; Kaim, W.; Schleid, T. Oxidative Perhydroxylation of $[\text{closo-B}_{12}\text{H}_{12}]^{2-}$ to the Stable Inorganic Cluster Redox System $[\text{B}_{12}(\text{OH})_{12}]^{2-/\cdot-}$: Experiment and Theory. *Chem. - Eur. J.* **2010**, *16*, 11242–11245. (m) Messina, M. S.; Axtell, J. C.; Wang, Y.; Chong, P.; Wixtrom, A. I.; Kirlikovali, K. O.; Upton, B. M.; Hunter, B. M.; Shafaat, O. S.; Khan, S. I.; Winkler, J. R.; Gray, H. B.; Alexandrova, A. N.; Maynard, H. D.; Spokoyny, A. S. Visible-Light-Induced Olefin Activation Using 3D Aromatic Boron-Rich Cluster Photooxidants. *J. Am. Chem. Soc.* **2016**, *138*, 6952–6955. (n) Ma, L.; Hamdi, J.; Wong, F.; Hawthorne, M. F. Closomers of High Boron Content: Synthesis, Characterization, and Potential Application as Unimolecular Nanoparticle Delivery Vehicles for Boron Neutron Capture Therapy. *Inorg. Chem.* **2006**, *45*, 278–285. (o) Lee, M. W., Jr. Catalyst-Free Polyhydroboration of Dodecaborate Yields Highly Photoluminescent Ionic Polyarylated Clusters. *Angew. Chem., Int. Ed.* **2017**, *56*, 138–142. (p) Qian, E. A.; Wixtrom, A. I.; Axtell, J. C.; Saebi, A.; Jung, D.; Rehak, P.; Han, Y.; Moully, E. H.; Mosallaei, D.; Chow, S.; Messina, M. S.; Wang, J. Y.; Royappa, A. T.; Rheingold, A. L.; Maynard, H. D.; Král, P.; Spokoyny, A. M. Atomically Precise Organomimetic Cluster Nanomolecules Assembled via Perfluoroaryl-Thiol S_2Ar Chemistry. *Nat. Chem.* **2016**, DOI: 10.1038/nchem.2686. (q) Hawthorne, M. F. The Role of Chemistry in the Development of Boron Neutron Capture Therapy of Cancer. *Angew. Chem., Int. Ed. Engl.* **1993**, *32*, 950–984. (r) Kultyshev, R. G.; Liu, J.; Liu, S.; Tjarks, W.; Soloway, A. H.; Shore, S. G. S-Alkylation and S-Amination of Methyl Thioethers - Derivatives of *closo*- $[\text{B}_{12}\text{H}_{12}]^{2-}$. Synthesis of a Boronated Phosphonate, *gem*-Bisphosphonates, and Dodecaborane-*ortho*-carborane Oligomers. *J. Am. Chem. Soc.* **2002**, *124*, 2614–2624. (s) Satapathy, R.; Dash, B. P.; Mahanta, C. S.; Swain, B. R.; Jena, B. B.; Hosmane, N. S. Glycoconjugates of Polyhedral Boron Clusters. *J. Organomet. Chem.* **2015**, *798*, 13–23. (t) Sivaev, I. B.; Bregadze, V. I.; Kuznetsov, N. T. Derivatives of the *closo*-Dodecaborate Anion and Their Application in Medicine. *Russ. Chem. Bull.* **2002**, *51*, 1362–1374. (u) Nakamura, H.; Ueda, N.; Ban, H. S.; Ueno, M.; Tachikawa, S. Design and Synthesis of Fluorescence-Labeled *closo*-Dodecaborate Lipid: Its Liposome Formation and *in vivo* Imaging Targeting of Tumors for Boron Neutron Capture Therapy. *Org. Biomol. Chem.* **2012**, *10*, 1374–1380.
- (5) General overview for Al, Ga, In, Tl: (a) Uhl, W. Tetrahedral Homonuclear Organoelement Clusters and Subhalides of Aluminum, Gallium and Indium. *Naturwissenschaften* **2004**, *91*, 305–319. (b) Linti, G.; Schnöckel, H.; Uhl, W.; Wiberg, N. Clusters of the Heavier Group 13 Elements. In *Molecular Clusters of the Main Group Elements*; Dreiss, M., Nöth, H., Eds.; Wiley-VCH: Weinheim, Germany, 2004; pp 126–168. For select Al clusters: (c) Dohmeier, C.; Robl, C.; Tacke, M.; Schnöckel, H. The Tetrameric Aluminum(I) Compound $[\{\text{Al}(\eta^5\text{-C}_5\text{Me}_5)_4\}]_4$. *Angew. Chem., Int. Ed. Engl.* **1991**, *30*, 564–565. (d) Purath, A.; Dohmeier, C.; Ecker, A.; Schnöckel, H.; Amelunxen, K.; Passler, T.; Wiberg, N. Synthesis and Crystal Structure of the Tetraaluminatetrahedrane $\text{Al}_4[\text{Si}(\text{t-Bu})_3]_4$, the Second Al_4R_4 Compound. *Organometallics* **1998**, *17*, 1894–1896. (e) Huber, M.; Schnöckel, H. $\text{Al}_4(\text{C}_5\text{Me}_5\text{H})_4$: Structure, Reactivity and Bonding. *Inorg. Chim. Acta* **2008**, *361*, 457–461. (f) Klinkhammer, K.-W.; Uhl, W.; Wagner, J.; Hiller, W. $\text{K}_2[\text{Al}_2\text{iBu}_{12}]$, a Compound with Al_2 Icosahedra. *Angew. Chem., Int. Ed. Engl.* **1991**, *30*, 179–180. For select Ga clusters: (g) Linti, G. On the Chemistry of Gallium. 6. Gallium(I) Tris(trimethylsilyl)silyl - an Experimental and Theoretical Study. *J. Organomet. Chem.* **1996**, *520*, 107–113. (h) Schnepf, A.;

Stoßer, G.; Schnöckel, H. The First Molecular Square Antiprismatic Ga₈ Cluster Exhibiting a *closo* Structure. *Z. Anorg. Allg. Chem.* **2000**, *626*, 1676–1680. (i) Wiberg, N.; Amelunxen, K.; Lerner, H.-W.; Nöth, H.; Ponikvar, W.; Schwenk, H. Silicon compounds. 122. Supersilyl Compounds of the Boron Group. 7. Tetrasupersilyl-tetrahedro-tetragallane (tBu₃Si)₄Ga₄ - a Tetrahedron with Especially Compact Ga₄ Tetrahedral Framework. *J. Organomet. Chem.* **1999**, *574*, 246–251.

(6) Schnöckel, H. Structures and Properties of Metalloid Al and Ga Clusters Open Our Eyes to the Diversity and Complexity of Fundamental Chemical and Physical Processes during Formation and Dissolution of Metals. *Chem. Rev.* **2010**, *110*, 4125–4163.

(7) *Boron Hydride Chemistry*; Muetterties, E. L., Ed.; Academic Press: New York, 1975.

(8) (a) Eberhardt, W. H.; Crawford, B.; Lipscomb, W. N. The Valence Structure of the Boron Hydrides. *J. Chem. Phys.* **1954**, *22*, 989–1001. (b) Longuet-Higgins, H. C.; de V. Roberts, M. The Electronic structure of the Borides MB₆. *Proc. R. Soc. London, Ser. A* **1954**, *224*, 336. (c) Longuet-Higgins, H. C.; de V. Roberts, M. The Electronic Structure of an Icosahedron of Boron Atoms. *Proc. R. Soc. London, Ser. A* **1955**, *230*, 110.

(9) Boone, J. L. Isolation of Hexahydro-*closo*-hexaborate (2-) Anion B₆H₆²⁻. *J. Am. Chem. Soc.* **1964**, *86*, 5036.

(10) Preetz, W.; Peters, G. The Hexahydro-*closo*-hexaborate Dianion [B₆H₆]²⁻ and Its Derivatives. *Eur. J. Inorg. Chem.* **1999**, *1999*, 1831–1846.

(11) (a) Baurmeister, J.; Franken, A.; Preetz, W. Preparation, ¹¹B NMR and Vibrational Spectra of Multialkylated *closo*-Hexaborates and Crystal Structures of *cis*- and *trans*-[P(C₆H₅)₄][B₆H₅(CH₃)₂] and *mer*-[P(C₆H₅)₄][B₆H₄(CH₃)₃]. *Z. Naturforsch.* **1995**, *50b*, 772–780. (b) Lübke, W.; Franken, A.; Preetz, W. Preparation, ¹¹B, ¹³C, ¹H NMR and Vibrational Spectra of 1,2-trimethylenepentahydro-*closo*-hexaborate(1-), *cis*-[B₆H₅(CH₂)₃]-, and 1,2-tetramethylenepentahydro-*closo*-hexaborate(1-), *cis*-[B₆H₅(CH₂)₄]-, and the Crystal Structures of [P(C₆H₅)₄][B₆H₅(CH₂)₃] and [P(C₆H₅)₄][B₆H₅(CH₂)₄]. *Z. Naturforsch.* **1994**, *49b*, 1115–1122. (c) Franken, A.; Preetz, W. Preparation, ¹¹B, ¹³C NMR and Vibrational Spectra of Cyanomethylhexahydro-*closo*-hexaborate(1-), [B₆H₆(CH₂CN)]⁻, and the Crystal Structure of [P(C₆H₅)₄][B₆H₆(CH₂CN)]. *Z. Naturforsch.* **1994**, *49b*, 471–476. (d) Lübke, W.; Preetz, W. Preparation, ¹¹B, ¹³C, ¹H NMR, and Vibrational Spectra of μ -methylene-*bis*-hexahydro-*closo*-hexaborate, [B₆H₆(CH₂)₂B₆H₆]²⁻ and Crystal Structures of [As(C₆H₅)₄]₂[B₆H₆(CH₂)₂B₆H₆].1/2(CH₃)₂CO. *Z. Naturforsch.* **1996**, *51b*, 545–550. (e) Heinrich, A.; Preetz, W. Preparation and Vibrational Spectra of Alkyl and Rhodano Hydrohexaborates. *Z. Naturforsch., B: J. Chem. Sci.* **1988**, *43b*, 1327–1331.

(12) Wixtrom, A. I.; Shao, Y.; Jung, D.; Machan, C. W.; Kevork, S. N.; Qian, E. A.; Axtell, J. C.; Khan, S. I.; Kubiak, C. P.; Spokoynny, A. M. Rapid Synthesis of Redox-Active Dodecaborane B₁₂(OR)₁₂ Clusters under Ambient Conditions. *Inorg. Chem. Front.* **2016**, *3*, 711–717.

(13) Kuznetsov, I. Y.; Vinitskii, D. N.; Solntsev, K. A.; Kuznetsov, N. T.; Butman, L. A. New Hydroboron Anion B₆H₇⁻. *Dokl. Akad. Nauk SSR* **1985**, *283*, 873–877.

(14) (a) Förster, D.; Scheins, S.; Luger, P.; Lentz, D.; Preetz, W. Electron Density and Bonding in Borates: An Experimental Study of Tetrabutylammonium Heptahydrohexaborate, [(C₄H₉)₄N][B₆H₇]. *Eur. J. Inorg. Chem.* **2007**, *2007*, 3169–3172. (b) Hofmann, K.; Proscen, M. H.; Albert, B. R. A New 4c–2e Bond in B₆H₇⁻. *Chem. Commun.* **2007**, *29*, 3097–3099. (c) Jacobsen, H. Hypovalency—A Kinetic-Energy Density Description of a 4c–2e bond. *Dalton Trans.* **2009**, *21*, 4252–4258. (d) Brint, P.; Healy, E. F.; Spalding, T. R.; Whelan, T. Bonding in Clusters. Part 3. Protonation of *nido*-Pentaborane(9), *nido*-Hexaborane(10), and *closo*-Hexaborate(6)(2-). *J. Chem. Soc., Dalton Trans.* **1981**, *12*, 2515–2522. (e) Cavanaugh, M. A.; Fehlner, T. P.; Stramel, R.; O'Neil, M. E.; Wade, K. Protonation of Cluster Molecules: Bridging Hydrogen Sites in Tetrahedral, Octahedral and Capped Square Pyramidal Clusters: Be₄H₈, B₄H₈, B₆H₇⁻ and B₆H₈ as Main Group Models for Transition Metal Cluster Systems. *Polyhedron* **1985**, *4*, 687–695. (f) Burkhardt, A.; Wedig, U.

von Schnering, H. G. The Electron Localization Function in *closo* Boron Clusters. *Z. Anorg. Allg. Chem.* **1993**, *619*, 437–441.

(15) (a) Steuer, B.; Peters, G.; Preetz, W. Alkyl Derivatives of [B₆H₆]²⁻: NMR and Vibrational Spectra and Crystal Structure of (Ph₄P)[B₆H₆CH₂Ph]. *Inorg. Chim. Acta* **1999**, *289*, 70–75. (b) Drewes, C.; Preetz, W. Synthesis, Spectra and Crystal Structure of *cis*-Monobenzylmononitrotetrahydro-*closo*-hexaborate(2-). *Z. Naturforsch., B: J. Chem. Sci.* **1999**, *54*, 1219–1221.

(16) (a) Baurmeister, J.; Franken, A.; Preetz, W. Preparation, Vibrational Spectra and Normal Coordinate Analysis of the D and ¹³C Isotopomers of the Methylpentahydro-*closo*-hexaborate [B₆H₅(CH₃)₂]²⁻ and the Crystal Structure of [P(C₆H₅)₄][B₆H₆(CH₃)]. *Z. Naturforsch.* **1995**, *50b*, 623–629.

(17) (a) Preetz, W.; Fritze, J. Preparation and Boron-11 NMR and Vibrational Spectra of the Octahedral *closo*-Borate Anions B₆X₆²⁻; X = Hydrogen, Chlorine, Bromine, or Iodine. *Z. Naturforsch.* **1984**, *39b*, 1472–1477. (b) Fritze, J.; Preetz, W.; Marsmann, H. C. *closo*-Halohydrohexaborate. II. Boron-11 NMR Spectra of the *closo*-Halohydrohexaborates X_nB₆H_{6-n}²⁻, n = 0–6; X = Cl, Br, I. *Z. Naturforsch.* **1987**, *42b*, 287–292. (c) Fritze, J.; Preetz, W. *closo*-Halohydrohexaborate. III. Vibrational Spectra of the *closo*-Halohydrohexaborates, X_nB₆H_{6-n}²⁻, n = 1–5; X = Cl, Br, I. *Z. Naturforsch.* **1987**, *42b*, 293–300. (d) Preetz, W.; Stallbaum, M. Preparation and Boron-11 NMR Spectra of the Perhalogenated *closo*-Hexaborates B₆X_nY_{6-n}²⁻, n = 0–6; X ≠ Y = Cl, Br, I. *Z. Naturforsch.* **1990**, *45b*, 1113–1117. (e) Thesing, J.; Stallbaum, M.; Preetz, W. Vibrational Spectra and Normal Coordinate Analysis of the Heteroleptic Halohexaborates B₆X_nY_{6-n}²⁻, n = 1–5; X ≠ Y = Cl, Br, I. *Z. Naturforsch.* **1991**, *46b*, 602–608.

(18) (a) Mesbah, W.; Soleimani, M.; Kianfar, E.; Geiseler, G.; Massa, W.; Hofmann, M.; Berndt, A. *hypercloso*-Hexa(amino)hexaboranes: Structurally Related to Known *hypercloso*-Dodecaboranes, Metastable with Regard to Their Classical Cycloisomers. *Eur. J. Inorg. Chem.* **2009**, *36*, 5577–5582. (b) Baudler, M.; Rockstein, K.; Oehlert, W. Tris(diethylamino)cyclotriborane and Constitutional Isomerism between *cyclo*- and *closo*-hexakis(diethylamino)hexaborane(6). *Chem. Ber.* **1991**, *124*, 1149–1152. (c) Siebert, W.; Maier, C.-J.; Greiwe, P.; Bayer, M. J.; Jofmann, M.; Pritzko, H. Small Boranes, Carboranes, and Heterocarboranes. *Pure Appl. Chem.* **2003**, *75*, 1277–1286.

(19) (a) Lorenzen, V.; Preetz, W.; Baumann, F.; Kaim, W. Paramagnetic Cluster Ions [B₆Hal_nHal'_{6-n}][•] (Hal, Hal' = Cl, Br, I). EPR Evidence for Radical Stabilization through Electronic Effects of the Halogen Substituents. *Inorg. Chem.* **1998**, *37*, 4011–4014. (b) Speiser, B.; Witzmann, T.; Würde, M. Two-Electron-Transfer Redox Systems, Part 7: Two-Step Electrochemical Oxidation of the Boron Subhalide Cluster Dianions B₆X₆²⁻ (X = Cl, Br, I). *Inorg. Chem.* **2003**, *42*, 4018–4028. (c) Wanner, M.; Kaim, W.; Lorenzen, V.; Preetz, W. Hexaborate Cluster Radical Anions [B₆Hal_nHal'_{6-n}][•] and [B₆Hal_nR][•] (Hal, Hal' = Cl, Br, I; R = H, alkyl). Chemical or Electrochemical Generation, Vibrational, UV-Vis and EPR Spectroscopy. *Z. Naturforsch.* **1999**, *54b*, 1103–1108.

(20) (a) Preetz, W.; Hake, M. G. Preparation and Boron-11 NMR and Vibrational Spectra of the *closo*-Hexaborates [B₆(SCN)₆]²⁻ and [B₆(SeCN)₆]²⁻. *Z. Naturforsch.* **1992**, *47b*, 1119–1121. (b) Preetz, W.; Steuer, B. Preparation, Vibrational Spectra, and Normal Coordinate Analysis of the ¹⁰B and ¹¹B Isotopomers of [B₂(NCS)₆]²⁻ and Crystal Structure of (Ph₃P=N=PPh₃)₂[B₂(NCS)₆]. *Z. Naturforsch.* **1996**, *51b*, 551–556.

(21) Blublitz, D.; Franken, A.; Preetz, W.; Thomsen, H. Preparation, ¹¹B NMR Spectra, Vibrational Spectra, and Normal Coordinate Analysis of *conjuncto-bis*-Hexahydro-*closo*-hexaborate, [B₆H₆-B₆H₆]²⁻, and the Crystal Structure of [P(C₆H₅)₄]₂-*conjuncto*-[B₆H₆-B₆H₆]. *Z. Naturforsch.* **1996**, *51b*, 609–618.

(22) (a) Wahab, A.; Douvris, C.; Klíma, J.; Šembera, F.; Ugolotti, J.; Kaleta, J.; Ludvík, J.; Michl, J. Anodic Oxidation of 18 Halogenated and/or Methylated Derivatives of CB₁₁H₁₂⁻. *Inorg. Chem.* **2017**, *56*, 269–276. (b) King, B. T.; Körbe, S.; Schreiber, P. J.; Clayton, J.; Némová, A.; Havlas, Z.; Vyakaranam, K.; Fete, M. G.; Zharov, I.; Ceremuga, J.; Michl, J. The Sixteen CB₁₁H_nMe_{12-n}⁻ Anions with

Fivefold Substitution Symmetry: Anodic Oxidation and Electronic Structure. *J. Am. Chem. Soc.* **2007**, *129*, 12960–12980.

(23) Preetz previously proposed an analogy between protonation of a facet of the hexaborate cage with formal cage oxidation, since in both cases cage bonding electron density is diminished and the overall cluster charge increases by one unit (2– to 1– or 1– to 0). See: Heinrich, A.; Keller, H.-L.; Preetz, W. Oxidation Reactions on $X_nB_6H_{6-n}^{2-}$, $X = Cl, Br, I$; $n = 1-6$, and Crystal Structures of $[(n-C_4H_9)_4N]B_6I_6$ and $[(n-C_4H_9)_4N]_2B_6I_6$. *Z. Naturforsch.* **1990**, *45b*, 184–190. This is relevant in the present case, given that **1a,b** are isolated as monoanionic species, each containing H^{fac} at one facet of the cage. Upon oxidation under electrochemical conditions, a neutral complex ($B_6(CH_2Ar)H^{fac}$) is likely generated; by Preetz's analogy, this would be comparable to a diprotonated hexaborate cluster. It has been well-established that the hexaborate core decomposes in the presence of strong acids (see ref 10) as a consequence of diprotonation and the resulting instability of this compound. Furthermore, the hypothetical diprotonated hexaborate cluster B_6H_8 has been evaluated computationally and was suggested to be unstable toward cage rupture (see, for example, ref 14d).

(24) (a) McKee, M. L. Density Functional Theory Study of Anionic and Neutral Per-Substituted 12-Vertex Boron Cage Systems, $B_{12}X_{12}^{n-}$ ($n = 2, 1, 0$). *Inorg. Chem.* **2002**, *41*, 1299–1305. (b) McKee, M. L.; Wang, Z.-X.; Schleyer, P. v. R. *Ab initio* Study of the *hypercloso* Boron Hydrides B_nH_n and $B_nH_n^-$. Exceptional Stability of Neutral $B_{13}H_{13}$. *J. Am. Chem. Soc.* **2000**, *122*, 4781–4793.

(25) Ong, C. W.; Huang, H.; Zheng, B.; Kwok, R. W. M.; Hui, Y. Y.; Lau, W. M. X-ray Photoemission Spectroscopy of Nonmetallic materials: Electronic Structures of Boron and B_xO_y . *J. Appl. Phys.* **2004**, *95*, 3527–3534.

(26) Kabbani, R. M. *Polyhedron* **1996**, *15*, 1951.